Journal of *Marine Science and Engineering*

MDPI

Article

Joint Optimization of Berth and Shore Power Allocation Considering Vessel Priority Under the Dual Carbon Goals

Yongfeng Zhang [1], Wenya Wang [2] and Houjun Lu [2,*]

[1] Shanghai International Shipping Institute, Shanghai Maritime University, Shanghai 201306, China; yfzhang@shmtu.edu.cn
[2] Logistics Engineering College, Shanghai Maritime University, Shanghai 201306, China; 202330210335@stu.shmtu.edu.cn
* Correspondence: hjlu@shmtu.edu.cn; Tel.: +86-021-38283356

Abstract

Against the backdrop of the dual-carbon strategy promoting the green and low-carbon transformation of the shipping industry, pollutant emissions generated during vessel berthing operations have become a critical challenge in port environmental governance. To address the combined effects of the priority berthing policy for new energy vessels and time-of-use electricity pricing, a joint optimization model for berth and shore power allocation is developed with the objectives of minimizing the total economic cost of vessels and the environmental tax cost associated with pollutant emissions. An improved Adaptive Large Neighborhood Search algorithm (ALNS-II) is further designed to solve the model. Numerical experiments based on actual port data verify the effectiveness of the proposed model and the superiority of the algorithm. The results indicate that, under time-of-use electricity pricing, the priority berthing policy for new energy vessels can shorten their waiting time at anchorage and encourage fuel-powered vessels to shift toward electrification. When the peak-to-valley electricity price ratio increases from 4.1:1 to 7.5:1, the environmental tax cost of pollutant emissions decreases slightly, whereas the total economic cost of vessels rises by 4.17%, suggesting that the peak-to-valley electricity price ratio should not be set excessively high. In addition, increasing the proportion of new energy vessels to 70% is more conducive to improving the overall economic and environmental performance of ports. The findings provide a theoretical basis and decision support for the optimal allocation of port resources under the coordination of multiple policies.

Keywords: dual-carbon goals; shore power; berth allocation; multi-energy vessels; berthing priority; bi-objective optimization

Check for updates

Academic Editor: Jinfen Zhang

Received: 10 March 2026
Revised: 30 March 2026
Accepted: 31 March 2026
Published: 7 April 2026

Copyright: © 2026 by the authors. Licensee MDPI, Basel, Switzerland. This article is an open access article distributed under the terms and conditions of the Creative Commons Attribution (CC BY) license.

1. Introduction

Shipping and ports are pivotal drivers of global trade and economic growth, accounting for approximately 80% of international trade volume and promoting economic cooperation. Automation has strengthened the competitiveness and efficiency of ports [1]. However, with the continuous growth of maritime activities, ports and their surrounding areas have gradually become major zones of energy consumption and pollution emissions. China has set ambitious targets to peak carbon emissions by 2030 and achieve carbon neutrality by 2060. Ports are among the primary sources of air pollution, with emissions mainly arising from handling operations and incoming vessels. Key measures include promoting the electrification of container terminals, supporting the application of shore

power technology for berthing vessels, and converting diesel-powered container cranes to electric operation. Shore power refers to the provision of onshore electricity to vessels during their berthing period, enabling them to shut down auxiliary engines, thus reducing fuel consumption and emissions. The approach serves as an effective measure for energy conservation and emission reduction, and is a key initiative in the development of green ports. The time-of-use (TOU) pricing policy, charging different electricity rates at different times, serves as a demand-side management tool with the continued growth of global electricity demand.

To further accelerate the development of low-carbon ports, the government has introduced a series of incentive policies, such as multi-energy powered vessels. It aims to gradually expand the application of green electricity, LNG, biodiesel, and green alcohol in the shipping sector. Incentives for new energy vessels include priority berthing and unberthing, such as partial reduction in berthing fees and preferential berth allocation. Consequently, ports need to account for the priority service of new energy vessels when formulating their berth allocation plans. However, under TOU pricing policies, new energy vessels may not necessarily choose to prioritize berthing. Currently, domestic shore power electricity pricing is beginning to implement the TOU mechanism, with peak, flat, and valley electricity price ratios reaching 1.5:1.0:0.3. This pricing structure means that if new energy vessels prioritize berthing and use shore power during peak electricity periods, they incur high electricity costs. Therefore, balancing priority berthing service for multi-energy powered vessels with the impact of TOU pricing policies has become a critical issue for port managers in advancing low-carbon ports.

1.1. Literature Review

The existing literature relevant to this study focuses on three main areas: ship priority, joint optimization of berth allocation and shore power, and TOU pricing. Vessel service priority has been recognized as an effective approach to improving port operational efficiency, and has been extensively studied in the existing literature [2–4]. Ganji et al. (2024) demonstrated that well-designed priority strategies can reduce vessel waiting times and enhance port operational efficiency [5]. Yıldırım et al. (2020) applied artificial bee colony optimization and simulation optimization techniques to solve flexible vessel priority management in container terminal berth allocation [6]. Chen et al. (2023) addressed a maritime rescue coverage problem by minimizing response time for heterogeneous rescue vessels [7]. Lu et al. (2025) presented an integrated model that incorporates tidal factors into the joint optimization of berth and quay crane operations, addressing both service standards and emissions during port stays and crane activities [8]. Ursavas et al. (2022) developed an efficient berth allocation decision support system by embedding a dynamic discrete event simulation model to determine berth allocation priorities for arriving vessels [9]. Considering uncertain vessel arrival time, Jiang et al. (2025) reviewed the corresponding prediction methods and influencing factors for maritime operational efficiency [10]. Wang et al. (2024) introduced an optimization method based on an active–reactive strategy for solving continuous berth allocation and quay crane allocation problems with mixed uncertainties [11]. The above studies provide valuable theoretical foundations and methodological insights for vessel priority scheduling.

Research on shore power primarily focuses on government subsidies, port optimization, and emission reduction benefits. Zhen et al. (2022a) compared two incentive policies on shore power system deployment, constructing a nonlinear programming model to optimize shore power deployment, berth allocation, and vessel service sequences [12]. Song et al. (2022) proposed that the government should prioritize subsidies for vessels using shore power to enhance the investment attractiveness of emission reduction technologies and optimize low-

carbon port operation paths [13]. Peng et al. (2019) studied the shore power allocation, aiming to minimize total shore power costs and carbon emissions, through determining the capacity expansion and usage patterns [14]. Zhang et al. (2025) developed a multi-objective optimization model for the coordinated allocation of shore power and berth scheduling, integrating economic benefits, environmental benefits, and operational efficiency [15].

In berth allocation research, Wang et al. (2020) considered carbon emission taxes, establishing a model aiming to minimize total completion delay costs and quay crane operational costs [16]. Rodrigues et al. (2022) and Zhen et al. (2022b) focused on the berth allocation problem that incorporates uncertainties like weather conditions, vessel arrival times, and container handling volumes [17,18]. Guo et al. (2024) explored a collaborative model for multiple terminals sharing shore-side and yard resources [19]. Zhang et al. (2022) considered a balance in port economic costs and environmental performance through the coordinated optimization of berth allocation and shore power assignment [20]. Wang et al. (2024) established a collaborative optimization model for berth allocation, quay crane, and shore power scheduling, which enhanced port throughput efficiency and service levels [21]. These studies collectively indicate that collaborative optimization of berth and shore power can reduce vessel waiting times and fuel consumption while balancing environmental protection and economic benefits.

The time-of-use (TOU) pricing mechanism has a significant impact on port energy scheduling costs, and some studies have begun to incorporate TOU pricing into optimization models. Parise et al. (2016) optimized the number of quay cranes operating during peak periods, reducing peak electricity demand by approximately 60% [22]. Van et al. (2018) achieved about a 10% electricity cost saving by limiting peak electricity demand for refrigerated containers in the yard. Some studies on collaborative scheduling of berths and terminal equipment have incorporated TOU pricing mechanisms [23]. Iris et al. (2021) proposed a mixed-integer linear programming model to address integrated operation planning and energy management issues considering different energy pricing schemes and bidirectional energy transactions between energy and storage systems [24]. Yu et al. (2022) studied the berth allocation and quay crane assignment problem (BACAP) to minimize electricity costs, delay times, and vessel emission costs, analyzing vessel costs under different TOU pricing [25]. The above studies take into account the practical characteristics of TOU pricing and are more aligned with the requirements of low-carbon port operations.

Table 1 summarizes literature related to joint optimization of berth and shore power allocation under TOU electricity pricing, considering vessel priority.

Table 1. Summary of the most related articles.

Paper	Berth Allocation	Shore Power Allocation	TOU Pricing	Objective	Solution Method
[4] Gao et al. (2025)	✓			Minimize ships' total stay time	GUROBI + ALNS
[5] Ganji et al. (2024)	✓			Minimize ship pollutant emissions	GAMS(38.2) + Simulation
[19] Guo et al. (2024)	✓	✓		Minimize total port operating cost	CPLEX + ALNS
[20] Zhang et al. (2022)	✓	✓		Minimize ship berthing cost and microgrid operation cost	CPLEX + Heuristic Algorithm
[21] Wang et al. (2024)	✓	✓		Minimize port operation cost, energy consumption, and total crane emissions	Adaptive Immune Clonal Selection Algorithm

Table 1. *Cont.*

Paper	Berth Allocation	Shore Power Allocation	TOU Pricing	Objective	Solution Method
[25] Yu et al. (2022)	✓	✓	✓	Minimize shore power usage cost, berthing delay, and carbon emissions	Meta-Heuristic Algorithm
This paper	✓	✓	✓	Minimizing the total economic costs of vessels and environmental tax costs from pollutant emissions	ALNS Algorithm

In summary, Existing research has made significant progress in the joint optimization of berth allocation and shore power scheduling, particularly in the application of multi-objective optimization models and meta-heuristic algorithms such as adaptive large neighborhood search (ALNS) and genetic algorithms (GA). These studies have effectively reduced vessel waiting times, energy consumption costs, and pollutant emissions, providing theoretical support for the development of green ports under the dual-carbon goals. For instance, some studies have incorporated carbon emission taxation into berth allocation models to balance operational efficiency and environmental costs, while others have explored the coordinated scheduling of berth resources and shore power systems under uncertainty. However, there are still some limitations in the existing research. First, the quantification of vessel priority rules requires further refinement. Most existing studies adopt fixed weight assignments, which fail to fully capture the dynamic influence of multiple factors, such as the remaining energy of new energy vessels and cargo handling volumes, on priority determination. Second, current research tends to examine either the impact of time-of-use (TOU) pricing or vessel priority on berth allocation in isolation, with limited efforts devoted to integrating these two factors within a unified framework. Finally, most studies focus on a single type of vessel, while the coexistence of heterogeneous vessels—such as fuel-powered, electric, and methanol-powered vessels—has received in-sufficient attention.

Therefore, this study investigates the joint optimization problem of berth allocation and shore power assignment under time-of-use (TOU) pricing while considering vessel priority. Multiple factors are comprehensively incorporated, including vessel types, TOU electricity pricing, berthing priority, shore power service coverage, safety distance constraints, and energy replenishment requirements. A bi-objective optimization model is developed to minimize the total economic cost of vessels and the environmental tax cost associated with pollutant emissions. To solve the model, an improved adaptive large neighborhood search (ALNS-II) algorithm is proposed. The results provide decision support for the coordinated optimization of berth allocation and shore power usage in the context of green port development.

1.2. The Contributions of This Paper

This paper addresses the joint allocation problem of berths and shore power in green port operations, with a particular focus on the simultaneous consideration of time-of-use (TOU) electricity pricing and vessel priority policies—a combination that has been largely overlooked in the existing literature. It compares and summarizes previous models and methods, identifying their limitations, especially the tendency to examine either TOU pricing mechanisms or vessel priority rules in isolation, as well as the insufficient treatment of heterogeneous vessel types and their distinct energy replenishment requirements. By incorporating TOU pricing, vessel priority rules,

multi-energy vessel characteristics, shore power service coverage, safety distance constraints, and energy replenishment processes into the modeling framework, the study improves upon these models, thereby establishing a more realistic and comprehensive bi-objective mixed-integer programming model. The objectives of this model are to minimize the total economic cost of vessels and the environmental tax cost associated with pollutant emissions. To solve this model, the study employs an improved adaptive large neighborhood search (ALNS-II) algorithm. This algorithm is designed to provide high-quality Pareto optimal solutions for berth and shore power allocation, outperforming traditional meta-heuristic methods such as multi-objective particle swarm optimization (MOPSO) and genetic algorithms (GA) in terms of solution quality, convergence, distribution uniformity, and diversity. Additionally, a sensitivity analysis of key parameters—including the peak-to-valley electricity price ratio, the proportion of new energy vessels, and vessel cost components—is conducted to assess the robustness of the proposed model under varying conditions and to provide decision support for port managers balancing economic and environmental objectives.

2. Problem Description and Model Formulations

2.1. Problem Description

Suppose a container terminal has B berths, each with dedicated quayside equipment. Currently, I vessels are scheduled to arrive, comprising three types: conventional fuel vessels, electric vessels, and methanol vessels. Under low-carbon incentive policies, electric and methanol vessels enjoy priority berthing rights. The time period is also divided into peak, flat, and valley segments with differentiated rates to incentivize shipowners to optimize berthing schedules and energy service plans based on TOU.

Vessel berthing priorities are given based on the following operational rules. Berthing is prioritized for new energy vessels, followed by fuel-powered vessels. For new energy vessels, those with lower remaining energy reserves receive priority berthing to promptly meet their energy replenishment needs. For vessels with the same type, those with larger cargo volumes receive priority berthing to enhance overall port operational efficiency. During berthing, energy usage varies by vessel type. Electric vessels must connect to shore power equipment for charging. Since shore power usage costs are influenced by TOU pricing policies, charging during off-peak hours is recommended to reduce expenses. Methanol vessels refuel at anchorages or berths, requiring maintenance of safe distances from adjacent vessels during refueling, as shown in Figure 1.

Under TOU pricing, effective coordination of berth allocation and shore power usage is essential to improving operational efficiency and reducing vessel-related emissions. This requires comprehensive consideration of practical constraints, including vessel types, arrival schedules, handling durations, service range, and capacity of shore power facilities. Moreover, port operations involve multiple stakeholders with differing objectives, where governments prioritize emission reduction, port authorities seek efficient resource utilization, and vessels aim to minimize wait costs. Therefore, this study investigates a joint berth and shore power allocation problem under realistic operational constraints, aiming to balance economic efficiency and environmental sustainability in low-carbon port operations.

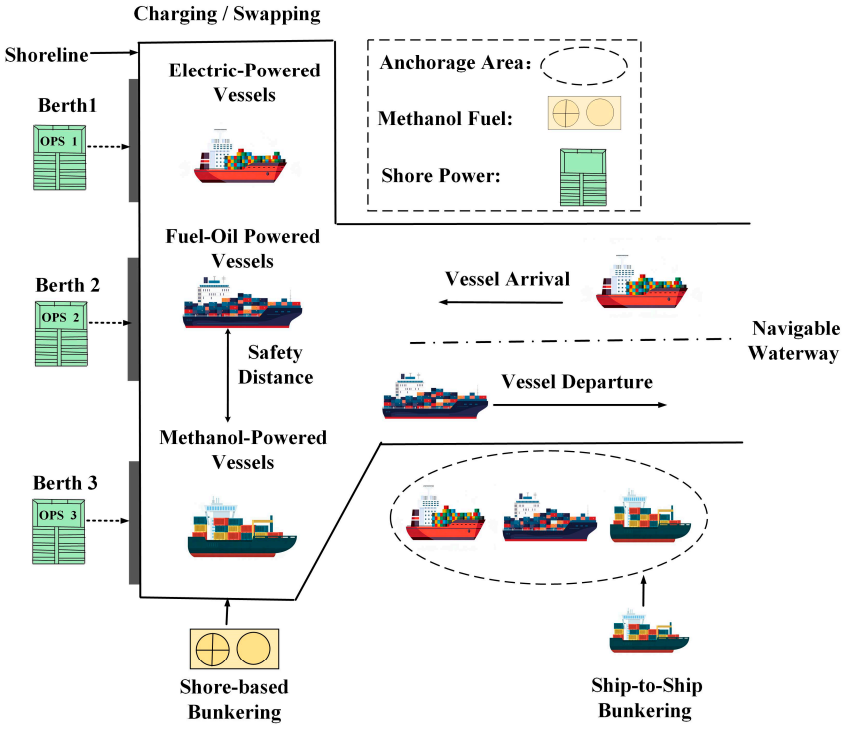

Figure 1. Vessel Operations Process in Port.

2.2. Model Formulations

2.2.1. Model Assumption Conditions

For the sake of simplicity and clarity of the model, the following key assumptions are made.

(1) Waterway conditions are assumed to consistently satisfy navigation requirements, ensuring that all vessels can safely access and depart from the terminal.
(2) The vessels' arrival time is known due to ships' time table, and the influence of weather, accidents and other interference on the vessels are not into consideration.
(3) All berths and shore power systems are assumed to be initially idle, ensuring a well-defined initial system state and avoiding the complexity associated with pre-existing allocations.
(4) The shore power connection time is assumed to be negligible compared to the vessel berthing and handling time.

2.2.2. Model Parameters and Definitions

To facilitate the model description, Table 2 presents the symbols used in the modeling process and their meanings.

Table 2. Notation definitions.

Set	Description
I	The set of vessels i during the planning period, $I = \{i = 1, 2, 3, \ldots, N\}$
B	The set of discretized continuous berths, $B = \{b = 1, 2, 3, \ldots, N\}$
T	Set of operational periods t within the planning period, T $= \{t = 1, 2, 3, \ldots, N\}$
P	Set of pollutants, P $= \{CO_2, SO_2, NO_2, PM_{2.5}\}$
V	Set of vessel types, V $= \{v = 1, 2, 3\}$ 1 = Electric vessels, 2 = Fuel vessels, 3 = Methane vessels
E	Set of shore power equipment, E $= \{e = 1, 2, 3 \ldots N\}$
K	Electricity period, K $= \{h, m, l\}$, where h = peak period, m = flat period, l = valley period

Table 2. *Cont.*

Set	Description
Parameters	
V_i	Vessel type i, $V_i \epsilon$V
Q_i	Cargo handling capacity of vessel i (tons)
l_i	Length of vessel i (m)
P_i^A	Engine power of vessel i (kW)
T_{ai}	Arrival time of vessel i (hours)
T_{zi}	Duration of berthing and cargo handling operations for Vessel i (hours)
E_{DTi}	Estimated departure time of vessel i (hours)
C_D	Diesel price ($/liter)
C_h	Peak Electricity Rate ($/kWh)
C_m	Flat electricity rate ($/kWh)
C_l	Valley electricity rate ($/kWh)
C_{Zi}	Delay Cost for Vessel i ($/hour)
C_{Mi}	Waiting cost for vessel i at anchorage ($/hour)
C_p	Pollutant p unit emission tax ($/kg)
D_e	Maximum power supply distance of shore power equipment (m)
d_{eb}	Distance from shore power equipment to berth (m)
l^A	Ship auxiliary machinery load factor
R^A	Ship auxiliary machinery diesel consumption rate (liters/kWh)
W_p	Pollutant p emission factor (kg/L)
A_1	Minimum shore power supply capacity (kW)
A_2	Maximum shore power supply capacity (kW)
L	Total shoreline length (m)
M	Sufficiently large positive number
D_s	Minimum safety distance for methanol vessels (m)
A_i	Selection of methanol vessel refueling sites
T_{ci}	Charging time required for electric vessel i (hours)
T_{gi}	Fueling time required for methanol vessel i (hours)
R_i	Remaining energy capacity of vessel i upon arrival at port (%)
ΔT	Priority time window (hours), set to 1 h
Auxiliary Variables	
U_{ij}	Binary, equal to 1 if berthing areas of ships i and j do not overlap; else 0
Z_{ij}	Binary, equal to 1 if the berthing time windows of vessels i and j do not overlap; else 0
σ_{ij}	Binary, equal to 1 if vessel i is prioritized over vessel j for berthing; else 0
α_{ij}	Binary, equal to 1 if the arrival time difference between new energy vessel i and fuel-powered vessel j is within ΔT; else 0
Decision Variables	
X_{ibt}	Binary, equal to 1 if Ship i docked at berth b at time t; else 0
Y_{ie}	Binary, equal to 1 if Ship i uses shore power equipment e; else 0
O_i	Binary, equal to 1 if Ship i uses shore power during berthing; else 0
T_{si}	Actual berthing time for vessel i
T_{fi}	Vessel i Actual Departure Time
T_{ih}	Duration of Ship's Electricity Consumption During Peak Pricing Period
T_{im}	Duration of electricity consumption by vessel i during flat periods
T_{il}	Duration of electricity consumption by vessel i during valley pricing periods
T_{wi}	Start time of charging for the electric vessel i
T_{ki}	Start time of the methanol vessels fuel replenishment

2.2.3. Mathematical Model

The model aims to minimize the total economic costs and environmental tax costs from pollutant emissions for all vessels, where the total economic cost primarily consists

of vessel time costs and energy consumption. Time costs for vessels, including anchorage waiting costs and delayed departure costs, are calculated as Equation (1).

$$C_{\mathrm{cw}} = \sum_{i\in I}\left(T_{fi} - E_{\mathrm{DT}i}\right) \times C_{Zi} + \sum_{i\in I}(T_{si} - T_{ai}) \times C_{Mi} (\forall i \in I) \tag{1}$$

Energy consumption costs encompass shore power usage fees and auxiliary genera tor fuel expenses, as provided in Equation (2). Shore power costs include TOU electricity rates across peak, flat, and valley periods. Auxiliary generator costs primarily reflect fuel expenditures for onboard power generation during berthing.

$$C_{\mathrm{mt}} = \sum_{i\in I}(C_h T_{ih} + C_m T_{im} + C_l T_{il}) l_A P_i^A O_i + \sum_{i\in I} C_D W_i^D (1 - O_i) \tag{2}$$

Beyond carbon emissions, this study also considers the environmental impacts of other pollutants such as SO_2, NO_x, and PM_x. Environmental taxes are imposed to uniformly quantify these pollutants as economic penalty costs. During berthing operations, if shore power is not utilized, diesel fuel must be consumed by auxiliary engines for power generation. Diesel consumption is calculated in Equation (3). The pollutant emissions from auxiliary diesel engines are calculated using Equation (4).

$$W_i^D = l^A P_i^A R^A T_{zi}, \forall i \in I \tag{3}$$

$$EM_i = W_i^D W_p, \forall i \in I \tag{4}$$

Thus, the objective functions of this model are provided as follows. Objective (5) minimizes the total economic cost of vessels. Objective (6) minimizes the environmental tax payment of pollutant emissions.

$$minF_1 = C_{mt} + C_{cw} \tag{5}$$

$$minF_2 = \sum_{i\in I}\sum_{p\in P} E\, M_i (1 - O_i) C_p, \forall i \in I, p \in P \tag{6}$$

$$\sum_{i\in I}\sum_{b\in B}\sum_{t\in T} X_{ibt} \le 1, i \in I, \forall b \in B, \forall t \in T \tag{7}$$

$$T_{fi} - T_{sj} \le M\left(1 - Z_{ij}\right),\ \forall i, j \in I, i \ne j \tag{8}$$

$$b_i + l_i \le b_j + M\left(1 - U_{ij}\right),\ \forall i, j \in I, i \ne j \tag{9}$$

$$Z_{ij} + Z_{ji} + U_{ij} + U_{ji} \ge 1,\ \forall i, j \in I, i \ne j \tag{10}$$

$$T_{si} \ge T_{ai}, \forall i \in I \tag{11}$$

$$\sum_{e\in E}\sum_{i\in I} Y_{ie} X_{ibt} \le 1, \forall e \in E, \forall i \in I, \forall t \in T \tag{12}$$

$$A_1 \le \sum_{i\in I} P_i^A Y_{ie} \le A_2, \forall t \in T, \forall e \in E \tag{13}$$

$$Y_{ie} d_{eb} \le D_e X_{ibt}, \forall i \in I, \forall e \in E, \forall b \in B, \forall t \in T \tag{14}$$

$$T_{ih} + T_{im} + T_{il} = T_{zi} O_i, \forall i \in I \tag{15}$$

$$\mathrm{T_{si}} \le \mathrm{T_{sj}} + \mathrm{M} \cdot \left(1 - \sigma_{\mathrm{ij}}\right) + \mathrm{M} \cdot \left(1 - \alpha_{\mathrm{ij}}\right), \forall \mathrm{i}, \mathrm{j} \in \mathrm{I}, \mathrm{i} \ne \mathrm{j}, \mathrm{V_i} \in \{1, 3\}, \mathrm{V_j} = 2 \tag{16}$$

$$\alpha_{ij} = \begin{cases} 1, & \text{if } \mid T_{ai} - T_{aj} \mid \le \Delta T \\ 0, & \text{otherwise} \end{cases} \tag{17}$$

$$T_{si} \le T_{sj} + M\left(1 - Z_{ij}\right), \forall i, j \in I, i \ne j, v_i = v_j, Q_i > Q_j \tag{18}$$

$$T_{si} \le T_{sj} + M\left(1 - Z_{ij}\right), \forall i, j \in I, i \ne j, Vi \in \{1, 3\}, R_i < R_j \tag{19}$$

$$X_{ibt} + X_{j,b-1,t} + X_{j,b+1,t} \le 1, \forall i \in I, V_i = 3, j \ne i, \forall b \in B, \forall t \in T \tag{20}$$

$$T_{ki} \le t \le T_{ki} + T_{gi}, \forall i \in I, V_i = 3, \forall t \in T \quad (21)$$

$$T_{fi} - T_{si} = T_{zi}, \forall i \in I, V_i = 2 \quad (22)$$

$$T_{wi} \ge T_{si}, \forall_i \in I, V_i = 1 \quad (23)$$

$$T_{fi} \ge Max(T_{si} + T_{zi}, T_{wi} + T_{ci}), \forall i \in I, V_i = 1 \quad (24)$$

$$T_{ki} \ge T_{si} - M(1 - A_i), \forall_i \in I, V_i = 3 \quad (25)$$

$$T_{ki} + T_{gi} \le T_{fi} + M(1 - A_i), \forall_i \in I, V_i = 3 \quad (26)$$

$$T_{ki} \ge T_{ai} - M \cdot A_i, \forall_i \in I, V_i = 3 \quad (27)$$

$$T_{ki} + T_{gi} \le T_{si} + M \cdot A_i, \forall_i \in I, V_i = 3 \quad (28)$$

Constraints (7) ensure that at any given time, each vessel can dock at only one berth, and each berth can accommodate only one vessel simultaneously. Constraints (8) ensure that vessels at the same berth must complete operations in the order of their arrival. Constraints (9) prohibit spatial overlap of vessels during berthing. Constraints (10) ensure that for any two vessels, both relationships in operation sequence and vertical offset are satisfied to prevent conflicts in time and space. Constraints (11) ensure that a vessel's actual berthing time is not earlier than its arrival time. Constraints (12) ensure that each vessel uses at most one shore power unit, and each shore power unit can supply power to only one vessel at a time. Constraints (13) ensure that the total power demand of all vessels using shore power is within the minimum and maximum power supply capacities of the port. Constraints (14) restrict shore power units to serving their designated berth and adjacent berths. Constraints (15) ensure that the total duration of electricity usage in each TOU pricing period for a vessel equals its total berthing time. Constraints (16) and (17) grant new energy vessels priority berthing rights within the effective time window, allowing them to berth before fuel-powered vessels. Constraints (18) ensure that among vessels of the same type, those with larger loading/unloading volumes have priority berthing rights. Constraints (19) ensure that among new energy vessels, those with lower energy reserves have higher berthing priority. Constraints (20) and (21) impose safety distance constraints on methanol vessels, ensuring that during the entire refueling process, no other vessels can berth within the safety distance range. Constraints (22) ensure that the actual departure time of a fuel-powered vessel equals its berthing time plus its loading/unloading duration. Constraints (23) ensure that electric vessels can only begin charging after berthing. Constraints (24) ensure that electric vessels can only depart after completing all necessary operations (loading/unloading, charging). Constraints (25) ensure that methanol vessels' refueling start time cannot be earlier than their berthing time. Constraints (26) ensure that methanol vessels' refueling must be completed before departure. Constraints (27) ensure that the refueling process of methanol vessels at anchorage must not start earlier than their arrival time. Constraints (28) ensure that the refueling of methanol vessels at anchorage is completed before vessel berthing.

3. Solution Method

This section designs a tailored heuristic algorithm for the abovementioned model based on the ALNS framework. Algorithm 1 presents the pseudocode for the improved ALNS-II algorithm. Here, S, S_0 and S^* denote the current solution, optimal solution, and temporary solution, respectively; W_d and W_r represent the weight vectors for destruction and restoration operations; θ_d and θ_r denote the real-time scores for destruction and restoration operators; π_d and π_r are operator scores; Ω^- and Ω^+ denote the method sets for destruction and restoration operations.

Algorithm 1: Pseudo-code for the improved ALNS-II algorithm

Input: Model parameters, maximum iteration count K_{max}, initial temperature T_0, cooling rate α, destruction ratio δ
Output: Pareto archive $\mathcal{A}$ (set of non-dominated solutions), best compromise solution
Initialization:
    Generate initial solution S_0 using heuristic rules S ← S_0, T ← T_0
    Initialize Pareto archive $\mathcal{A} \leftarrow \{S_0\}$
    Initialize destruction operator weights $W_d \leftarrow [0.25, 0.25, 0.25, 0.25]$
    Initialize repair operator weights $W_r \leftarrow [0.33, 0.33, 0.34]$
    Initialize operator scores $\pi_d \leftarrow 0$, $\pi_r \leftarrow 0$
    Initialize operator usage counters $\theta_d \leftarrow 0$, $\theta_r \leftarrow 0$
Main Loop:
    for k = 1 to K_{max} do
        Select destruction operator d $\in \Omega^-$ based on weights W_d
        Select repair operator r $\in \Omega^+$ based on weights W_r
        $\theta_d \leftarrow \theta_d + 1$, $\theta_r \leftarrow \theta_r + 1$
        S′ ← Apply destruction operator d to S (remove $\xi \cdot |I|$ vessels)
        S′ ← Apply repair operator r to reconstruct S′
        Compute objective values $F_1(S')$ and $F_2(S')$ using Equations (5) and (6)
        //Multi-Objective Acceptance Criterion
        if S′ dominates S (i.e., $F_1(S') \leq F_1(S)$ and $F_2(S') \leq F_2(S)$, with at least one strict inequality) then
            S ← S′
            Update operator scores $\pi_d \leftarrow \pi_d + 30$, $\pi_r \leftarrow \pi_r + 30$
        else if S′ is not dominated by S then
            $\Delta\min \leftarrow \min \{F_1(S') - F_1(S), F_2(S') - F_2(S)\}$
            if exp $(-\Delta\min/T) >$ random (0,1) then
                S ← S′
                Update operator scores $\pi_d \leftarrow \pi_d + 15$, $\pi_r \leftarrow \pi_r + 15$
            else
                Update operator scores $\pi_d \leftarrow \pi_d + 5$, $\pi_r \leftarrow \pi_r + 5$
            end if
        end if
        //Pareto Archive Update
        if S′ is not dominated by any solution in $\mathcal{A}$ then
            Add S′ to $\mathcal{A}$
            Remove from $\mathcal{A}$ any solution dominated by S′
        end if
        //Adaptive Weight Update
        Update destruction operator weights $W_d \leftarrow (1 - r)\, W_d + r\, (\pi_d / \theta_d)$
        Update repair operator weights $W_r \leftarrow (1 - r)\, W_r + r\, (\pi_r / \theta_r)$
        T ← αT
    end for
Return: Pareto archive $\mathcal{A}$ and best compromise solution (closest to origin)

3.1. Initial Solution Generation

The initial solution generation strategy is designed based on heuristic rules. First, vessels are sorted by their arrival time T_{ai}. Then, berths b and operation times t are sequentially assigned to each vessel, ensuring compliance with berth length constraints and spatiotemporal uniqueness constraints. This initial solution comprises the decision variable set $V = \{X, Y, T, O\}$, where $X = \{X_{ibt} | X_{ibt} \in \{0, 1\}\}$ denotes the spatiotemporal allocation

matrix indicating whether vessel i occupies berth b at time t, and $Y = \{y_{ie} | y_{ie} \in \{0,1\}\}$ denotes the matching relationship matrix indicating whether vessel i uses shore power equipment e, $T = \left\{t_{si}, t_{fi}\right\}$ records the actual berthing and unberthing times of vessels, and $O = \{O_i | O_i \in \{0,1\}\}$ represents the decision variable for whether vessels use shore power. The algorithm employs a multi-level nested dictionary data structure, balancing data integrity and operational efficiency.

It should be noted that the initial solution generated by the above heuristic serves only as a starting point for the ALNS-II algorithm. The assignment decision for each vessel i can be expressed as:

$$\text{assign}(i) = \arg \min_{b \in \mathcal{B},\, t \geq T_{ai}} \{t : \text{feasible}(i, b, t)\} \tag{29}$$

where $\mathcal{B}$ denotes the set of berths, T_{ai} is the arrival time, and $\text{feasible}(i, b, t)$ indicates that vessel i can be moored at berth b from time t without violating any constraints. This greedy, earliest-available-time rule mimics the common first come first served practice in port operations, providing a feasible and reproducible baseline.

3.2. Design of Destruction and Repair Operators

The proposed algorithm has four types of disruption operators and three types of restoration operators to construct new solutions, tailored to the characteristics of the berth and shore power allocation.

The algorithm employs four destruction operators to remove selected vessels from the current solution, controlled by a destruction ratio $\xi \in (0,1)$. Let I denote the set of all vessels, and let $I_{assigned} \subseteq I$ be the set of vessels currently assigned in the solution.

(1) Random destruction operator. Randomly selects $\left\lceil \xi \mid I_{assigned} \mid \right\rceil$ vessels uniformly from $I_{assigned}$ and removes their allocations from the current solution. This operator ensures diversity in the search.

(2) Worst-case destruction operator. Computes a cost contribution C_i for each vessel $i \in I_{assigned}$ based on the current composite objective:

$$C_i = \omega_1 \cdot C_i^W + \omega_2 \cdot C_i^E + \omega_3 \cdot C_i^D \tag{30}$$

where C_i^W, C_i^E, and C_i^D denote the waiting cost, energy cost, and delay cost of vessel i, respectively. The weights $\omega_1, \omega_2, \omega_3$ are dynamically adjusted according to the current Pareto archive. The vessels with the highest C_i values are selected for destruction until $\left\lceil \xi \mid I_{assigned} \mid \right\rceil$ vessels are removed.

(3) Correlation disruption operator. This operator targets vessels that are temporally correlated with a randomly selected seed vessel. Let i_0 be a randomly chosen vessel from $I_{assigned}$. The set of vessels to be destroyed is defined as:

$$\mathcal{D}_{corr} = \left\{ j \in I_{assigned} : \mid T_{sj} - T_{si_0} \mid \leq \varepsilon \right\} \tag{31}$$

where T_{si} is the actual berthing time of vessel i, and ε is a predefined overlap threshold (set to 0.5 h in this study). If $\mid \mathcal{D}_{corr} \mid < \left\lceil \xi \cdot \mid I_{assigned} \mid \right\rceil$, additional vessels are randomly selected from $I_{assigned} \setminus \mathcal{D}_{corr}$ to meet the destruction ratio.

(4) Time-slot disruption operator. This operator focuses on vessels that berth during peak electricity tariff periods. Let $\mathcal{P}$ denote the set of time intervals corresponding to peak periods (e.g., 9:00–12:00 and 19:00–22:00). The set of vessels to be destroyed is defined as:

$$\mathcal{D}_{time} = \left\{ i \in I_{assigned} : T_{si} \in \mathcal{P} \right\} \tag{32}$$

If $|\mathcal{D}_{\text{time}}| < \lceil \xi \cdot |I_{\text{assigned}}| \rceil$, additional vessels are randomly selected from $I_{\text{assigned}} \setminus \mathcal{D}_{\text{time}}$ to satisfy the destruction ratio.

After applying a destruction operator, the removed vessels are stored in a list of unassigned vessels, which will be re-inserted by the subsequent repair operator.

The algorithm employs three repair operators to reassign the vessels removed by the destruction operator. Each operator constructs a feasible allocation for the unassigned vessels in sequence.

(1) Greedy repair operator. For each unassigned vessel, the operator evaluates all feasible berth-time combinations (b, t) that satisfy the spatial and temporal constraints. The combination with the smallest incremental contribution to the composite objective F is selected.

(2) Regret-based repair operator. This operator calculates a regret value for each unassigned vessel to avoid locally myopic decisions. The regret value r_i for vessel i is defined as:

$$r_i = \Delta_{i,2} - \Delta_{i,1} \tag{33}$$

where $\Delta_{i,1}$ and $\Delta_{i,2}$ are the first- and second-best objective improvements achievable by assigning vessel i to its best feasible berth-time combination. Vessels with higher regret values are assigned first, followed by the greedy assignment for the remaining vessels.

(3) Random repair operator. For each unassigned vessel, this operator randomly selects a feasible berth-time combination (b, t) from the set of all feasible combinations, with uniform probability. This operator enhances solution diversity.

Figure 2 illustrates an example of the aforementioned operator addressing a berth allocation problem involving 3 berths and 5 vessels. Each vessel corresponds to a set of available berths, where 1 indicates the vessel can berth at the corresponding berth and 0 indicates it cannot. The break-fix operator randomly adjusts the strategy, changing the assigned berths for Vessels 1, 2, and 4 from Berths 2, 1, and 3 to Berths 2, 1, and 2.

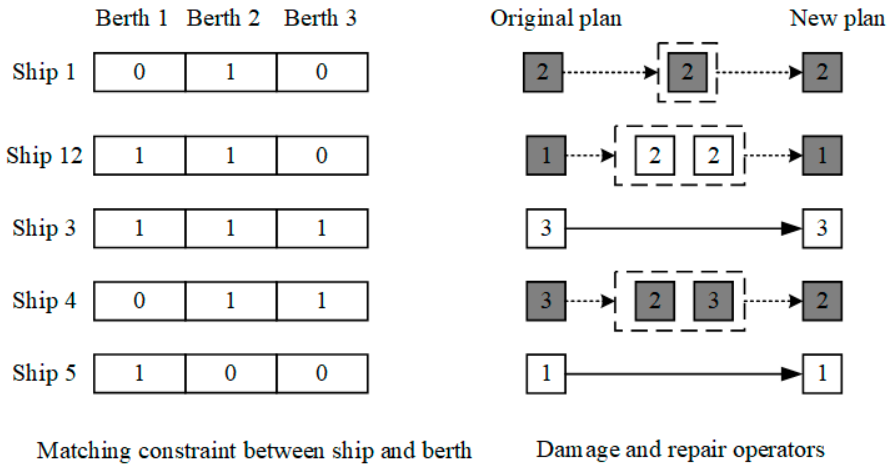

Figure 2. Example of Berth Allocation Operator.

3.3. Adaptive Mechanism

The adaptive mechanism of this algorithm primarily manifests in the dynamic adjustment of weights for the disruption and repair operators. The weights W_k for each operator are updated via the equation $W_k^{(t+1)} = (1 - r) \cdot W_k^t + r \cdot \pi_k^t$, where r is the response factor ($0 < r < 1$), and π_k^t represents the operator's performance score at iteration t. Specifically, when an operator combination generates a new optimal solution, it receives the highest score ($\pi_k^t = 30$); if it produces a solution superior to the current one, it receives the next-highest score ($\pi_k^t = 15$); even if it only generates a solution close to the current one, it still receives a base score ($\pi_k^t = 5$). Through this scoring mechanism, the algorithm dynami-

cally updates the selection probabilities of each operator, enabling operators with superior performance to gain more application opportunities. This achieves self-optimization and dynamic equilibrium of the operator combinations.

3.4. Acceptance Criteria and Termination Conditions

The acceptance criterion employs a simulated annealing-based mechanism with an acceptance probability. This mechanism permits acceptance of suboptimal solutions during the early search phase. As the temperature updates according to the cooling rate, the algorithm progressively shifts toward accepting only superior solutions.

The proposed algorithm employs multiple criteria. It stops when any of the following occurs: reaching the maximum iteration count, failing to improve for consecutive iterations, dropping below a specific temperature threshold, and exceeding the predefined computation time. This design of multiple termination conditions ensures the algorithm has sufficient search time while avoiding excessive computational resource consumption during ineffective searches.

3.5. Multi-Objective Handling Strategy

The proposed ALNS-II algorithm addresses the bi-objective optimization problem using a Pareto-based approach. Unlike weighted-sum methods that combine multiple objectives into a single scalar function, the algorithm maintains an external archive of non-dominated solutions throughout the search process, allowing it to directly approximate the Pareto frontier. The multi-objective mechanism consists of three key components:

First, a pareto dominance check. Given the current solution S and a candidate solution S', we evaluate both objectives F_1 (total economic cost of vessels) and F_2 (environmental tax cost of pollutant emissions). If S' dominates S, i.e., with at least one strict inequality, the candidate is unconditionally accepted.

$$F_1(S') \leq F_1(S) \text{ and } F_2(S') \leq F_2(S) \tag{34}$$

Next, non-dominated acceptance criterion. If neither solution dominates the other, the candidate may be accepted with a probability that depends on the current temperature, allowing the algorithm to explore the trade-off region. Following common practice in multi-objective simulated annealing, the acceptance probability is defined as:

$$P = \exp(\frac{\Delta_{\min}}{T}) \tag{35}$$

where $\Delta_{\min} = \min\{F_1(S') - F_1(S),\ F_2(S') - F_2(S)\}$ and T is the current temperature. This formulation encourages movement toward the Pareto front while permitting occasional acceptance of solutions that improve one objective at the expense of the other.

Finally, pareto archive maintenance. All non-dominated solutions encountered during the search are stored in an external archive $\mathcal{A}$. After each iteration, the archive is updated as follows: If the candidate solution S' is not dominated by any solution in $\mathcal{A}$, it is added to $\mathcal{A}$. Any solution in $\mathcal{A}$ that is dominated by S' is removed. At the termination of the algorithm, the set $\mathcal{A}$ constitutes the approximate Pareto frontier.

The flowchart of the ALNS-II algorithm is shown in Figure 3. First, initialize the ALNS-II parameters and weights, and generate an initial feasible solution. Then, enter the iterative loop to select and apply the destruction and repair operators based on weights, compute the objective value of the candidate solution, update the current solution and check for optimality based on whether the new solution is accepted. Simultaneously, update the operator weights until the maximum iteration count is reached, then return the optimal solution.

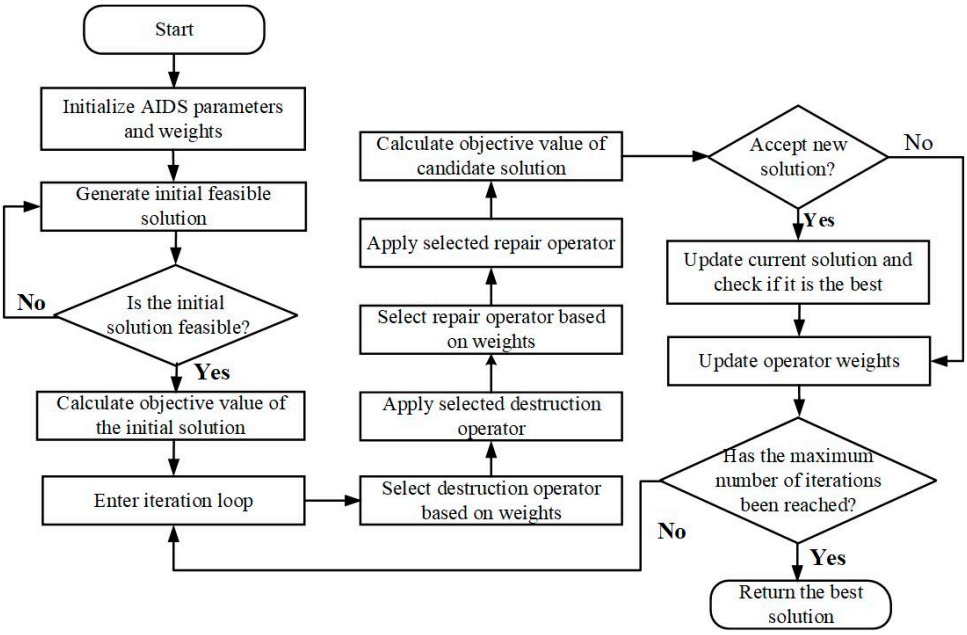

Figure 3. Flow chart of the ALNS-II Algorithm.

3.6. Comparison with Classical ALNS

To highlight the novelty of the proposed ALNS-II algorithm, Table 3 summarizes the key differences between the classical ALNS framework and our improved version.

Table 3. Comparison between classical ALNS and the proposed ALNS-II algorithm.

Aspect	Classical ALNS	Proposed ALNS-II
Objective	Single-objective	Bi-objective (Pareto-based)
Acceptance criterion	Simulated annealing based on single objective improvement	Pareto dominance check + non-dominated acceptance probability
Pareto archive	Not maintained	External archive $\mathcal{A}$ stores all non-dominated solutions; updated after each iteration
Destruction operators	Random, worst-cost (general purpose)	Random, worst-cost, correlation disruption, time-slot disruption
Correlation disruption	–	Destroys vessels with overlapping berthing times:
Time-slot disruption	–	Destroys vessels berthing during peak tariff periods
Repair operators	Greedy (general purpose)	Greedy, regret-based, random
Regret-based repair	–	Prioritizes vessels with higher regret
Adaptive weight update	Based on single objective improvement scores	Based on multi-objective scores
Operator weights	Adjust according to the historical scores dynamically	The same mechanism, but the scores are derived from multi-objective scoring

Compared with the classical ALNS framework, the proposed ALNS-II algorithm incorporates several key improvements: (i) a Pareto-based multi-objective handling strategy with a dominance-based acceptance criterion and an external archive; (ii) two problem-specific destruction operators (correlation disruption and time-slot disruption) that exploit the temporal structure of berthing schedules; (iii) a regret-based repair

operator to avoid myopic decisions; and (iv) an adaptive weight update mechanism that uses multi-objective scores.

4. Numerical Experiments

4.1. Experiment Settings

This section designs a case study based on data from a container terminal to validate the effectiveness of the proposed model and algorithm. The berthing length is 1500 m for vessels with three berths equipped with shore power facilities. TOU electricity rates are shown in Table 4. The planning cycle spans from 8:00 AM to 8:00 PM the following day at a container terminal. During this period, 12 vessels arrive at the port, including 4 fuel-powered, 4 electric, and 4 methanol-powered vessels. Detailed vessel information is provided in Table 5. The unit time cost for vessel waiting and the unit cost for delay are calculated as $1000l_i/2760$ and $2000l_i/2760$ respectively [26]. Other parameters are determined based on actual terminal data and literature references. Referencing China's fuel market, the average diesel price is 7.2 \$/kg. The diesel emission factors for SO_2, NO_2, PM_{10}, and $PM_{2.5}$ are listed in Table 6. Currently, there is no unified pricing policy for these pollutants. Their equivalent values relative to CO_2 are 0.95, 0.95, 0.28, and 2.28, respectively. The equivalent value auxiliary machinery load factor is 0.5, with auxiliary machinery fuel consumption rate at 0.2 L/kWh. The carbon tax rate is 2.66 \$/kg. Numerical experiments are implemented on a laptop equipped with an Intel Core@ 1.60 GHz processor and 32 GB of memory, running through the PyCharm 2023.2.1 plat form.

Table 4. TOU pricing.

Time Period	Electricity Price/($/kWh)	Time Period
Peak Period	1.15	9:00 AM–12:00 PM, 7:00 PM–10:00 PM
Flat Period	0.55	8:00 AM–9:00 AM, 12:00 PM–7:00 PM, 10:00 PM–12:00 AM
Valley Period	0.37	0:00 AM–8:00 AM

Table 5. Ship Parameters.

Vessel ID	Length /m	Vessel Type	Arrival Time	Estimated Departure Time	Loading/ Unloading Time (h)	Delay Cost ($)	Waiting Cost ($)	Loading/ Unloading Volume (TEU)	Energy Reserve (%)	Charging Time (h)	Refueling Time (h)
1	123	Fuel	08:18	19:00	10	89.13	44.57	900	35	0	0
2	119	Electric	08:45	17:00	8	86.23	43.12	730	34	9	0
3	113	Methanol	08:58	18:00	8	81.88	40.94	780	27	0	8.6
4	115	Fuel	11:14	21:30	9	83.33	41.67	880	26	0	0
5	95	Electric	16:35	22:40	6	68.84	34.42	580	35	5	0
6	105	Methanol	19:55	4:55	7	76.09	38.04	620	38	0	8
7	106	Fuel	20:27	06:00	8	76.81	38.41	860	22	0	0
8	89	Electric	20:34	03:00	5	64.79	32.25	450	23	6	0
9	93	Methanol	21:00	05:00	6	67.39	33.70	540	31	0	5
10	138	Fuel	22:10	10:40	12	100.00	50.00	950	26	0	0
11	96	Electric	21:35	6:00	8	69.57	34.78	750	37	8.5	0
12	95	Methanol	23:48	8:30	8	68.84	34.42	720	36	0	8

Table 6. Fuel Oil Vessel Emission Factors.

Emitted Pollutants	CO_2	SO_2	NO_2	PM_{10}	$PM_{2.5}$
Emission Factor	0.308	0.00002	0.0468	0.0014	0.0014

The ALNS-II algorithm proposed in this paper consists of 12 parameters, including the number of iterations, cooling rate, operator weights, and acceptance criteria-related parameters. To determine the appropriate parameter configuration, this paper adopts the Irace automatic parameter configuration framework. Twelve representative examples are selected as the parameter tuning sample set, and the parameter space is searched during 30 generations of iterations. Each parameter configuration is evaluated by running the ALNS-II algorithm, and the single run time is limited to 5 min. The final parameter settings were those identified as the optimal combination by Irace. The parameter value range and the final results are shown in Table 7.

Table 7. Algorithm Parameter Configurations.

Symbol	Description	Minimum	Maximum	Optimal Value
η	Maximum Iterations	500	5000	1000
T	Initial temperature (simulated annealing)	1000	100,000	50,000
α	Temperature cooling rate	0.90	0.999	0.995
ϱ	Failure rate parameter	0.1	0.3	0.2
π_{k1}^{t}	New Optimal Solution Reward Weight	20	50	30
π_{k2}^{t}	Better Solution Reward Weight	10	30	15
π_{k3}^{t}	Acceptable Solution Reward Weight	1	10	5
P	Acceptance Probability Parameter	0.15	0.25	0.2
d_1	Random Destruction of Initial Weights	0.1	0.4	0.25
d_2	Correlated initial weight perturbation	0.1	0.4	0.25
d_3	Initial weight for the time period damage	0.1	0.4	0.25
d_4	Worst-case disruption initial weight	0.1	0.4	0.25
r_1	Greedy Repair Initial Weight	0.2	0.6	0.33
r_2	Regret value correction initial weight	0.2	0.6	0.33
r_3	Randomly restore initial weight	0.2	0.6	0.33

4.2. Results and Analysis of Numerical Examples

The distribution of Pareto optimal solutions obtained using the improved ALNS-II algorithm is shown in Figure 4, where each solution corresponds to a specific joint berth–shore power allocation scheme. Terminal operators can select an appropriate scheduling plan according to practical requirements. In this study, a balanced solution between total economic cost and environmental tax cost of pollutant emissions is selected, corresponding to the Pareto optimal solution closest to the origin in Figure 4 (red point). The resulting berth–shore power allocation scheme is illustrated in Figure 5. The horizontal axis represents time, and the vertical axis represents discrete berth indices. Within each berth, vessels are vertically stacked to indicate their temporal sequence; the vertical position does not represent their physical location along the quay, as each berth is treated as an independent unit. The red bars indicate peak electricity tariff periods, while the yellow bars represent the waiting time of vessels at anchorage after arrival but before berthing. Each rectangle corresponds to the berthing time interval of a vessel, where the first line denotes the vessel ID and the second line indicates the identifier of the shore power unit used.

The corresponding solution is shown in Figure 4. In the berth-shore power allocation scheme, electric vessels (1, 4, 7, 11) and methanol vessels (3, 6, 9, 12) must decide whether to prioritize berthing. Electric vessel 4 and methanol vessel 9 opted for priority berthing but did not use shore power. Meanwhile, methanol vessel 6 and electric vessel 7 arrived during peak electricity pricing periods. Although they met the berth and shore power usage criteria, they did not immediately prioritize berthing operations. Instead, they waited until the next lower-cost pricing period (flat or valley period) to commence operations.

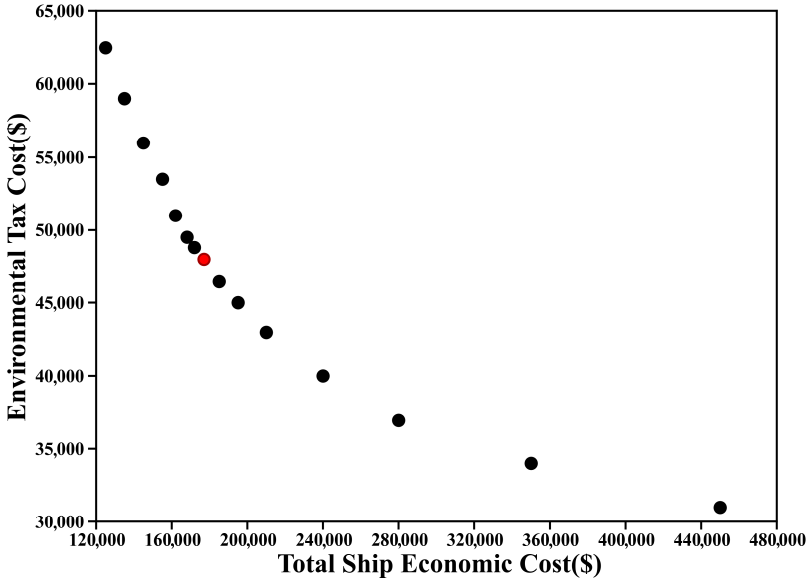

Figure 4. Pareto Frontier Distribution.

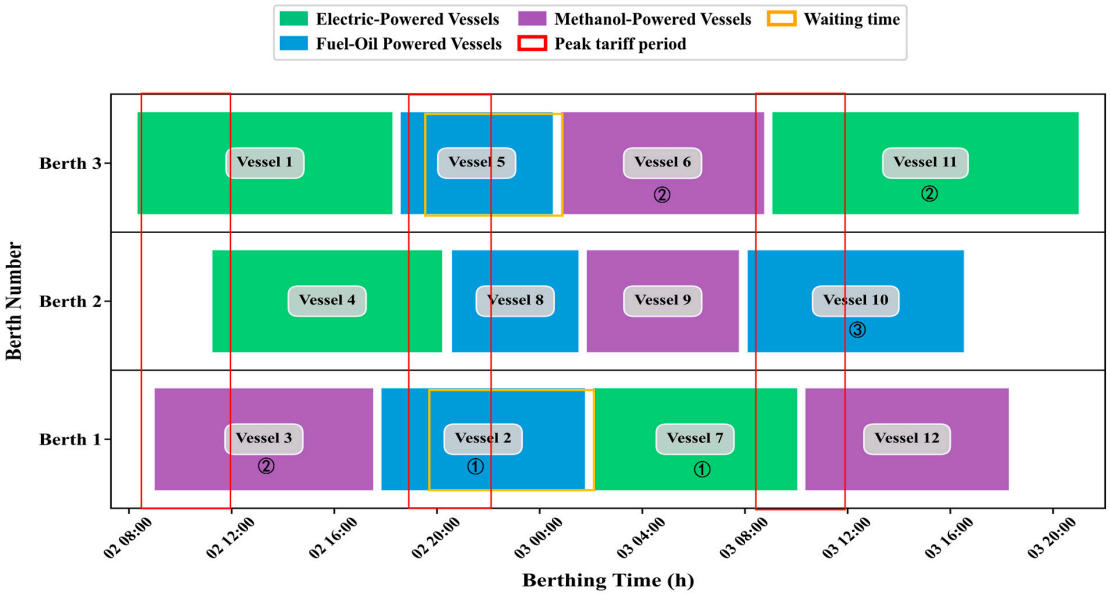

Figure 5. Gantt Chart of the Pareto Optimal Berth Shore Power Allocation Plan.

The decision on whether methanol vessel 6 and electric vessel 7 should be prioritized for berthing will impact fuel vessels 2 and 5. Four scenarios were designed for comparison, as shown in Table 8. Analysis reveals that if Vessel 6 forgoes priority berthing, it avoids peak electricity costs, reducing shore power usage costs by 76.71% and total economic costs by 51.04%. However, it incurs delay and waiting costs associated with anchoring for 1.48 h. If electric vessel 7 chooses priority berthing, it avoids anchorage waiting but operates during peak electricity pricing, increasing shore power costs by 303.32% and total economic costs by 64.24%. Therefore, both new energy vessels prefer to forgo priority berthing to reduce shore power costs. This decision simultaneously impacts the cost structure of fuel vessels. The total economic cost of fuel vessel 5 decreases by 65.49%, whereas that of fuel vessel 2 increases by 27.01%.

Table 8. Comparison of cost changes in the priority berthing strategy.

Vessel Decision Scenario	Affected Vessel	Shore Power Usage Cost ($)	Vessel Delay Cost ($)	Vessel Waiting Cost ($)	Total Economic Cost ($)
Scenario A	Methanol Vessel 6	5635.62	1118.75	0	6753.37
	Fuel Vessel 5	0	1584.23	1336.36	2920.59
Scenario B	Methanol Vessel 6	1312.41	936.57	1058.41	3306.39
	Fuel Vessel 5	0	1007.56	0	1007.76
Scenario C	Electric Vessel 7	5228.45	1204.13	0	6432.58
	Fuel Vessel 2	2668.31	1356.73	1376.62	5400.56
Scenario D	Electric Vessel 7	1296.34	1372.42	1248.13	3916.49
	Fuel Vessel 2	3107.56	1145.61	0	4252.17

Although prioritizing berthing for new energy vessels can reduce anchorage waiting time under a TOU pricing mechanism, it may also increase their overall economic costs. Consequently, new energy vessels can choose whether to prioritize berthing based on the cost–benefit analysis. Moreover, providing priority berthing to new energy vessels increases waiting costs for other fuel-powered vessels. This cost pressure will enhance the incentive for fuel-powered vessels to retrofit and adopt shore power.

To validate the model against real-world operations, we compare it with the terminal's current scheduling practice, which follows a simple first-come-first-served(FCFS) rule and does not consider the joint optimization of berth and shore power allocation, time-of-use electricity pricing, or vessel priority policies. The comparison results are presented in Table 9.

Table 9. Comparison between model decisions and terminal's FCFS scheduling practice.

Objective Function Value	FCFS Baseline	Proposed Model	Improvement
Total Economic Cost ($)	225,438.52	183,245.76	23.03%
Environmental Tax Cost ($)	62,723.15	51,648.23	21.44%

Compared with the FCFS baseline, the proposed joint optimization model for berth and shore power allocation, which simultaneously accounts for time-of-use electricity pricing and vessel priority, reduces the total economic cost by an average of 23.03% and the environmental tax cost by an average of 21.44%. This result demonstrates that the model effectively captures the operational trade-offs introduced by time-of-use pricing and vessel priority, achieving synergistic improvements in both economic and environmental performance while enhancing resource utilization efficiency, thereby providing actionable decision support for terminal managers.

4.3. Algorithm Performance

This section evaluates the ALNS-II algorithm from two aspects of effectiveness and superiority. Comparative experiments are conducted with the GUROBI solver, Multi-objective Particle Swarm Optimization (MOPSO), and Genetic Algorithm (GA).

4.3.1. Algorithm Effectiveness Analysis

To evaluate the effectiveness and scalability of the proposed ALNS-II algorithm, we compare it against the GUROBI solve. When the GUROBI optimal solution is known, the gap is calculated as $(\text{ALNS-II} - \text{GUROBIOptimal})/\text{GUROBIOptimal} \times 100\%$. When only a lower bound is available, the gap is computed as $(\text{ALNS-II} - \text{GUROBILower bound})/\text{GUROBILower bound} \times 100\%$. This dual definition ensures a fair and transparent comparison across all instance scales. The objective function values and running times obtained by GUROBI and the algorithm are presented in Table 10.

Table 10. Comparison Results Between the ALNS-II Algorithm and the GUROBI.

INS	Total Economic Cost ($)				Environmental Tax Cost ($)			
	GUROBI	ALNS-II	GAP (%)	GUROBI Running Time (s)	GUROBI	ALNS-II	ALNS-II Running Time (s)	GAP (%)
B4_S18_P4	186,382.52	186,382.52	0.00%	219	52,453.95	52,453.95	10	0.00%
B4_S21_P4	195,218.93	195,218.93	0.00%	288	53,690.21	53,690.36	13	0.00%
B4_S24_P4	197,892.31	198,255.45	0.18%	174	55,218.75	55,418.23	15	0.36%
B4_S27_P4	204,126.13	205,079.53	0.47%	440	57,640.36	57,880.27	19	0.42%
B4_S30_P4	210,653.83	211,424.63	0.37%	356	58,482.42	58,693.42	23	0.36%
B4_S33_P4	221,989.54	223,493.52	0.68%	691	59,690.96	60,038.46	27	0.58%
B5_S36_P5	232,914.76	234,712.63	0.77%	157	62,694.25	63,067.46	29	0.60%
B5_S39_P5	236,782.49	239,186.36	1.02%	1215	65,603.46	66,211.48	48	0.93%
B5_S42_P5	246,317.56	248,562.59	0.91%	2624	67,723.52	68,302.51	61	0.85%
B5_S45_P5	249,932.43	253,028.18	1.24%	2072	71,994.21	72,920.36	78	1.29%
B5_S48_P5	256,684.82	258,329.64	0.64%	6258	73,684.05	74,315.34	98	0.86%
B5_S51_P5	289,066.48	290,217.34	0.40%	1980	74,824.15	75,214.66	103	0.52%
B5_S54_P5	297,926.35	299,371.56	0.49%	3634	75,573.48	76,122.52	120	0.73%
B6_S57_P6	307,025.62	309,937.71	0.95%	2079	76,917.36	77,939.03	146	1.33%
B6_S60_P6	—	315,292.83	1.15% †	10,800	—	78,243.68	167	1.52% †
B6_S63_P6	—	329,980.45	1.32% †	10,800	—	81,437.81	182	1.78% †
B6_S66_P6	—	332,965.61	1.08% †	10,800	—	82,269.45	196	1.45% †
B6_S69_P6	—	349,950.32	1.21% †	10,800	—	86,479.07	217	1.60% †
B6_S72_P6	—	351,314.96	0.94% †	10,800	—	88,974.86	228	1.27% †
B6_S75_P6	—	382,919.37	1.45% †	10,800	—	89,381.46	242	1.93% †

Note: "—" indicates that GUROBI failed to obtain a feasible solution within the time limit. "†" indicates that the GAP is calculated based on the best lower bound obtained by GUROBI.

The experimental results indicate that as the problem size increases, the solver's computation time grows exponentially. For the smaller instances, GUROBI successfully finds the optimal solution, but its running time increases rapidly. For the larger instances, GUROBI fails to find a feasible solution within the 10,800s time limit. In contrast, the improved ALNS-II algorithm designed in this paper completes the solution within 250 s for all test cases. For the instances where GUROBI finds the optimal solution, ALNS-II yields objective values with an average gap of less than 1.5%. For the larger instances where GUROBI fails to return a feasible solution, ALNS-II produces solutions that lie within 2.0% of the best lower bound provided by GUROBI. Therefore, the ALNS-II algorithm provides efficient and effective solutions for the proposed problem.

4.3.2. Algorithm Comparisons

To further validate the superiority of the ALNS-II algorithm, three algorithms were compared across different scales. Each scale included 10 test instances, and each algorithm was run 10 times per instance. Four metrics were used for comparison: Pareto Optimality Distance (DPO), Extended Spread (ES), Number of Pareto Solutions (NPS), and Inverse Generation Distance (IGD). For IGD, a reference Pareto front is required. Since the true front is unknown, the reference is constructed by merging all non-dominated solutions from all three algorithms across all runs for each instance, and then removing dominated solutions. Figure 6 shows the distribution of these metrics for the solution sets generated by the three algorithms.

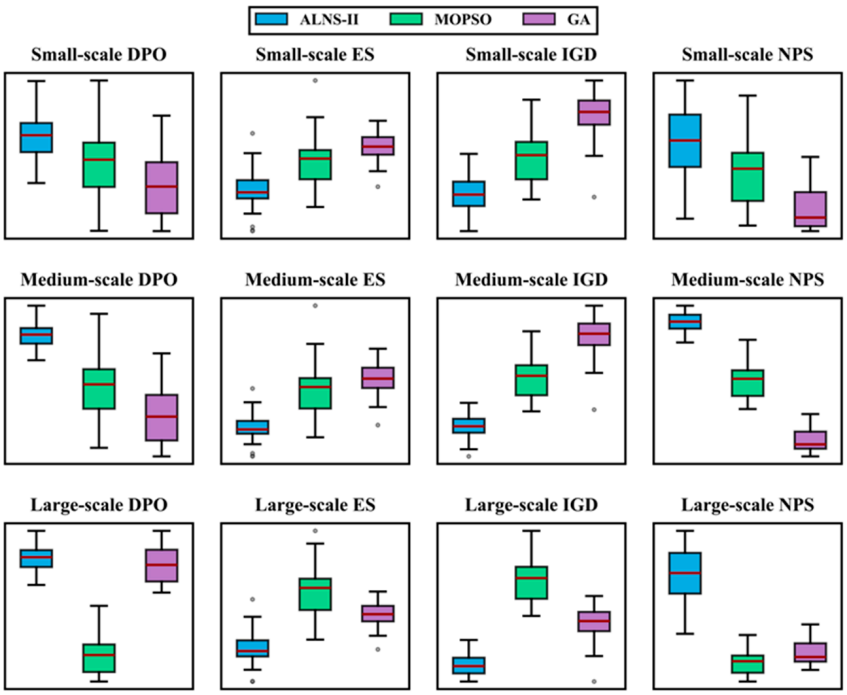

Figure 6. Boxplots of DPO, ES, IGD, and NPS from three algorithm solutions.

In terms of the DPO metric, the box position of the ALNS-II algorithm is significantly higher than that of MOPSO and GA, indicating that the Pareto solutions obtained by ALNS-II have the highest quality. For the ES metric, the box position of the ALNS-II algorithm is lower than that of the other two algorithms, suggesting that its solution set is more evenly distributed. Regarding the IGD metric, the overall distribution of the ALNS-II algorithm is clearly superior to MOPSO and GA, reflecting better convergence performance and a closer proximity to the true Pareto front. For the NPS metric, the box position of the ALNS-II algorithm significantly leads the other algorithms, demonstrating its ability to achieve a larger number of non-dominated solutions. Furthermore, from the distribution characteristics of the boxes, the data distribution of the ALNS-II algorithm across all metrics is relatively compact, showcasing good algorithm stability and consistency. This fully validates the comprehensive advantages of the ALNS-II algorithm in terms of solution quality, convergence, uniformity, and the number of solutions.

4.4. Sensitivity Analysis

This section explores how the berth and shore power optimization model can adapt its decision-making strategies in response to variations in electricity prices, changes in the number of renewable energy vessels, and shifts in vessel operating costs.

4.4.1. Impact of Electricity Pricing Mechanisms

Electricity price is a key factor influencing shore power costs. This study compares a uniform pricing scheme (fixed at 0.75 $/kWh) with a TOU pricing scheme. Using the base prices of these two schemes as reference points, two additional scenarios were generated by adjusting hourly prices by 5% upward and 5% downward, respectively. The impact of different pricing schemes on the total economic cost of vessels was analyzed. Figure 7 presents the comparison of total economic costs for vessels under different pricing scenarios. The TOU pricing scheme consistently yields the lowest total economic cost for vessels, while the flat rate scheme results in higher costs. Moreover, a 5% fluctuation in electricity prices significantly impacts the total economic costs.

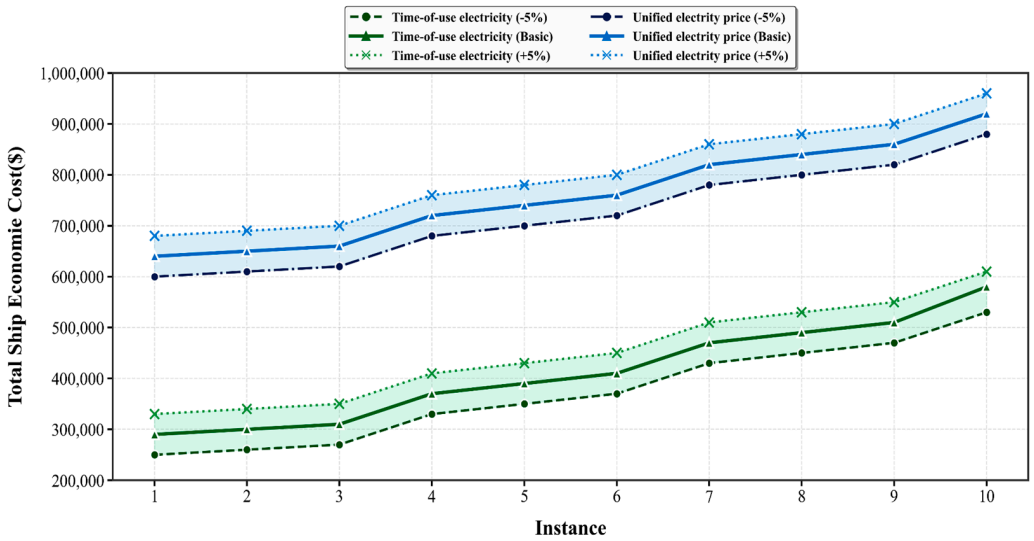

Figure 7. Sensitivity Analysis of Different Electricity Pricing Schemes.

To achieve the objective of peak shaving, the current TOU pricing adjustment strategy typically widens the price differential between peak and off-peak periods. This means increasing electricity rates during peak hours, while reducing them during valley hours. Peak rates are increased by 30%, valley rates are decreased by 20%, and intermediate rates are adjusted by 10%. The peak-to-off-peak price differential will be incrementally increased, with the specific adjustment plan detailed in Table 11.

Table 11. TOU Rate Floating Adjustment.

Floating Scheme	TOU Pricing Adjustment Strategy	Electricity Price/[($·(kWh))]	Peak-Valley Price Differential
1	Peak Electricity Price Reduced by 30% Valley electricity rates increased by 30%	Peak: 0.81, flat: 0.69, Valley: 0.36	2.25:1
2	Peak electricity rates reduced by 20% Valley electricity rates increased by 20%	Peak: 0.92, flat: 0.69, Valley: 0.34	2.71:1
3	Peak electricity rates reduced by 10% Valley electricity rates increased by 10%	Peak: 1.04, flat: 0.69, Valley: 0.31	3.35:1
4	Electricity rates unchanged	Peak: 1.15, flat: 0.69, Valley: 0.28	4.11:1
5	Peak electricity rates increased by 10% Valley electricity rates reduced by 10%	Peak: 1.27, flat: 0.69, Valley: 0.25	5.08:1
6	Peak electricity rates increased by 20% Valley electricity rates reduced by 20%	Peak: 1.38, flat: 0.69, Valley: 0.22	6.27:1
7	Peak electricity rates increased by 30% Valley electricity rates reduced by 30%	Peak: 1.50, flat: 0.69, Valley: 0.20	7.50:1

Figure 8 shows the results of different peak-off-peak electricity pricing strategies. As the peak-off-peak electricity price differential gradually increases, the environmental tax cost of pollutant emissions from the berth-to-shore power allocation scheme exhibits a decreasing trend. This indicates that widening the peak-off-peak price differential can effectively reduce pollutant emissions, while the total economic costs for vessels continue to rise simultaneously.

The cost trends for new energy vessels and fuel-powered vessels are shown in Figure 9. As the peak-off-peak electricity price differential gradually increases, the shore power usage costs for both new energy vessels and fuel-powered vessels show a decreasing trend, which may impact the promotion and application of shore power. When the peak-off-peak price differential exceeds 4.11:1, the delay costs for new energy vessels begin to rise gradually,

while those for fuel vessels continue to decrease. This indicates that in the scheduling scheme, more new energy vessels choose not to prioritize berthing to avoid peak electricity prices, while fuel-powered vessels gain priority berthing opportunities. Therefore, to prevent adverse scheduling incentives and preserve the effectiveness of the priority berthing policy for new energy vessels, port authorities should consider maintaining the peak-to-valley price ratio at or below 4.11:1, where environmental benefits and economic costs reach a practical balance.

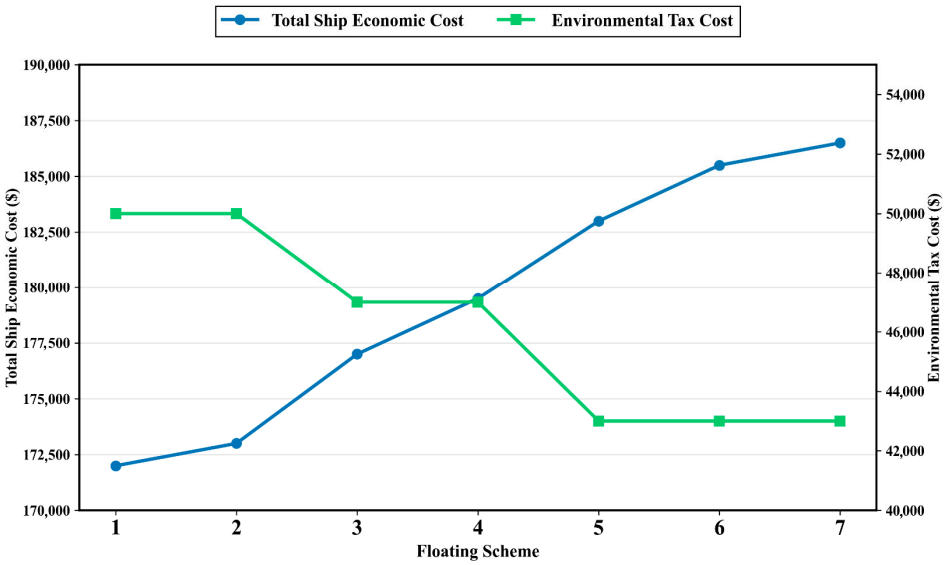

Figure 8. Sensitivity Analysis of TOU Pricing.

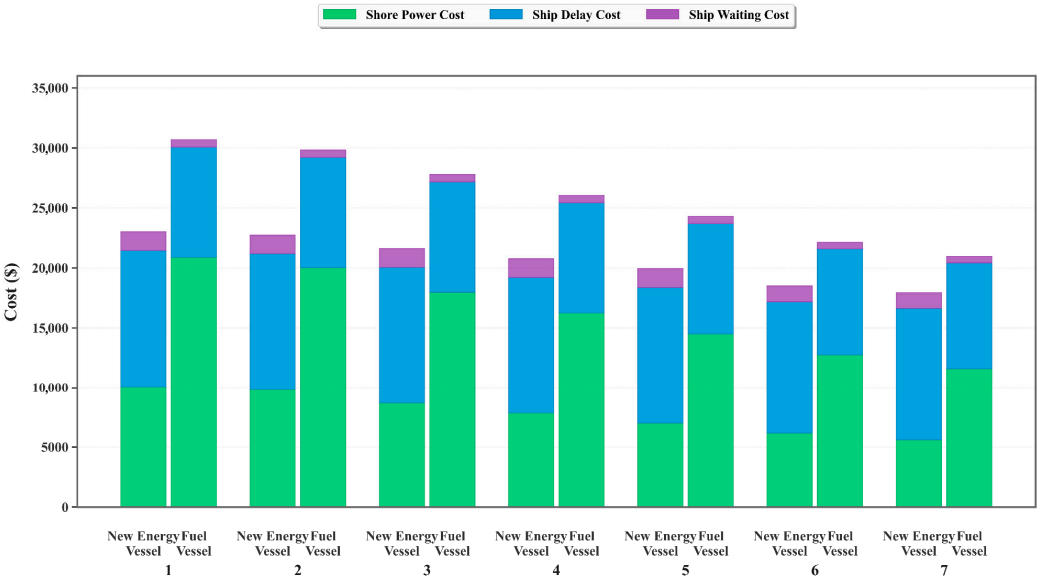

Figure 9. Ship Operator Costs Under Different Electricity Price Fluctuations.

4.4.2. Impact of New Energy Vessel Proportions

To analyze the impact of new energy vessel ratios on port operations, this section designs nine distinct scenarios, each corresponding to a different proportion of new energy vessels. Based on a 48 h operational scenario involving 30 vessel arrivals, the analysis investigates how new energy vessel ratios influence port economic and environmental benefits, as shown in Table 12.

Table 12. Comparison of Allocation Schemes for Different New Energy Vessel Ratios.

Example	New Energy Vessels Ratio (%)	Ship Time Cost ($)	Energy Consumption Cost ($)	Total Ship Economics Cost ($)	Pollutant Emissions Environmental Tax Cost ($)
1	10	101,169.26	85,213.46	188,373.28	65,829.35
2	20	101,713.46	90,487.15	195,394.36	64,921.48
3	30	102,167.44	95,642.78	197,356.24	62,793.62
4	30	102,373.15	100,328.91	202,496.35	61,836.63
5	50	102,784.76	105,791.23	208,164.38	59,374.45
6	60	102,913.76	110,255.37	211,424.63	58,693.42
7	70	103,159.82	115,638.49	218,423.25	57,104.55
8	80	103,272.52	120,472.56	223,386.32	56,280.35
9	90	104,907.21	125,186.84	228,459.36	54,391.24

The research results show that when the proportion of new energy vessels increases from 10% to 90%, the vessel time cost increases by 3.69%, while the environmental tax cost from pollutant emissions and energy consumption cost decrease by 17.38% and 31.93%, respectively. This is because, in addition to the routine loading and unloading tasks, new energy vessels require additional energy replenishment during berthing, which increases their berth occupancy time. At the same time, the use of shore power or clean fuel by new energy vessels significantly reduces pollutant emissions, leading to a decrease in environmental tax costs from pollutant emissions. Therefore, a proportion of 70% new energy vessels is more conducive to improving both the economic and environmental performance of ports. Therefore, a proportion of 70% new energy vessels is more conducive to improving both economic and environmental performance. Beyond this point, the environmental benefits start to diminish, while economic costs continue to rise. At 70%, the port achieves an optimal balance, where the reduction in emissions outweighs the increased operational costs, maximizing overall performance.

4.4.3. Impact of Vessel Costs

To analyze the impact of cost-related parameters on berth and shore power allocation schemes, vessels' costs of waiting, deviation, and delay were increased by 50% from their original levels while keeping other parameters constant. Table 13 indicates that waiting costs constitute a component of the overall operating expenses.

Table 13. Impact of Vessel Waiting and Delay Costs on Results.

Cost Item	Baseline ($)	Waiting Cost Increased by 50%	Difference from Benchmark Difference/%	Delay Cost Increased by 50%	Compared to Baseline Difference/%
Total Economic Cost per Vessel ($)	177,061.75	23,826.48	34.77%	189,256.65	6.89%
Environmental Tax Cost Pollutant Emission ($)	48,089.70	56,483.50	17.46%	50,997.30	6.05%
Vessel Time Cost ($)	108,386.65	125,233.43	15.54%	112,761.35	4.04%
Ship Energy Consumption Cost ($)	68,675.10	83,393.05	21.46%	71,495.30	4.11%

Delay costs exert a lesser influence on total vessel economic costs, as terminal operational efficiency necessitates maintaining vessel delays within reasonable limits, resulting in minimal variation in delay levels. The most significant factor affecting vessel energy costs

is waiting costs. When waiting costs increase, vessels reduce their electricity consumption during off-peak hours, consequently raising vessel energy costs.

4.4.4. Impact of Carbon Tax Pricing Mechanisms

Carbon tax is a widely used policy instrument to internalize the environmental cost of emissions. Currently, there is no unified carbon tax pricing policy; therefore, analyzing the impact of different carbon tax structures on the model's outcomes is essential. Consider two carbon tax functions: a single-rate tax and a tiered (piecewise) tax.

The single-rate tax applies a constant rate to all emissions, defined as:

$$C_2^{CT}(z) = r_0 z \tag{36}$$

where z denotes the total carbon emissions, and r_0 is the constant tax rate. In this study, r_0 is set to 2.66 \$/kg.

The tiered tax adopts a piecewise linear structure, where the tax rate increases progressively with emissions, as given in Equation (37):

$$C_2^{CT}(z) = \begin{cases} z \cdot x_1, & 0 < z \leq z_1 \\ z \cdot x_2 + b_1, & z_1 < z \leq z_2 \\ z \cdot x_3 + b_2, & z > z_2 \end{cases} \tag{37}$$

In the formula: The tax rates x_1, x_2, and x_3 are 1.36 \$/kg, 2.71 \$/kg, and 5.43 \$/kg re spectively. z_1 and z_1 are 10,000 and 15,000 kg respectively. The comparison between the two carbon tax schemes is presented in Table 14.

Table 14. Comparison of single-rate and tiered carbon tax schemes.

Metric	Single-Rate Tax	Tiered Tax
Total Pollutant emissions volume (kg)	23,580.13	18,920.04
Vessels using shore power (ID)	2,3,6,7,10,11	1,2,4,7,8,9,10,12
Shore power cost (\$)	5635.62	31,731.52
Pollutant emission environmental tax cost (\$)	62,723.15	50,617.58

The results show that the tiered carbon tax scheme leads to a 20.9% reduction in total Pollutant emissions volume compared to the single-rate scheme, while pollutant emission environmental tax cost decreases by 19.3%. This indicates that the tiered structure, which imposes higher rates on larger emitters, provides a stronger incentive for vessels to reduce emissions, particularly by shifting to shore power. Notably, the number of vessels using shore power increases from six under the single-rate scheme to eight under the tiered scheme, demonstrating the effectiveness of progressive carbon pricing in promoting cleaner energy adoption.

5. Discussion

This section summarizes and discusses the key findings and insights from a management perspective, demonstrating the practical significance and applicability of this study. In terms of trade-off analysis and decision support, the bi-objective optimization model presented in this study offers a Pareto optimal solution set, facilitating a balanced coordination between economic and environmental performances. Port managers can make informed decisions based on their strategic priorities: selecting solutions with lower total costs when emphasizing economic efficiency or opting for those with reduced pollution costs when prioritizing environmental responsibility.

In terms of the coordination mechanism for TOU pricing policies, as shown in Figure 8, when the peak-to-valley price ratio increased from 2.25:1 to 4.11:1, the delay costs for new energy vessels rose by 6.12%. and when the peak-to-valley differential further increased from 4.1:1 to 7.5:1, the delay cost surge significantly expanded to 25.92%. This indicates that as the peak-off-peak price differential widens, more new energy vessels forgo priority berthing to avoid peak-hour electricity rates, contradicting the original intent of promoting priority berthing policies for new energy vessels. Therefore, it is recommended that government departments, when formulating TOU pricing policies, comprehensively consider coordination with the priority berthing policy for new energy vessels. The peak-off-peak electricity price differential should be controlled within 4.1:1 to prevent negative interactions between policies.

Regarding infrastructure investment and resource allocation, increasing the proportion of new energy vessels from 10% to 90% reduces environmental tax costs for pollutant emissions by 17.38%, reflecting the significant emission-reduction effect of new energy adoption. However, vessel time costs correspondingly increase by 3.69%. Therefore, port managers should consider the actual number of new energy vessels arriving daily and the service capacity to deploy shore power and energy supply facilities.

6. Conclusions

This study addresses the berth and shore power allocation problem considering the TOU pricing and vessel priority. A bi-objective optimization model is developed to minimize both the total economic costs of vessels and the environmental tax costs of pollutant emissions, while balancing economic and environmental benefits at the terminal. The improved ALNS-II algorithm is designed to solve the model, and its effectiveness is validated through empirical analysis. Experimental results demonstrate the superiority of the proposed algorithm in terms of solution quality, distribution uniformity, solution diversity, and algorithm convergence, particularly for medium- and large-scale cases. Sensitivity analysis revealed that lower electricity prices reduce vessels' energy consumption costs and environmental tax costs, while increasing the number of vessels using shore power. Although a higher share of new energy vessels significantly decreases pollutant emissions, it may increase vessels' waiting costs. Therefore, port authorities should set electricity prices and plan shore power investments by jointly considering operational impacts, emission reductions, and service capacity.

However, this study does not explicitly account for the impact of stochastic factors, such as uncertainty in vessel arrival times, non-negligible shore power connection times, and fluctuations in electricity demand. Future research could extend this work by developing robust or stochastic optimization models that incorporate uncertainties in vessel arrivals and the non-instantaneous nature of shore power connection processes. In addition, further studies may explore integrated scheduling frameworks that combine shore power systems with smart grids, energy storage technologies, and renewable energy sources.

Author Contributions: Writing—original draft preparation, W.W.; writing—review and editing, H.L. and Y.Z. All authors have read and agreed to the published version of the manuscript.

Funding: This research received no external funding.

Data Availability Statement: The original contributions presented in this study are included in the article. Further inquiries can be directed to the corresponding author.

Conflicts of Interest: The authors declare no conflicts of interest.

References

1. Yu, H.; Huang, M.; He, J.; Tan, C. The clustering strategy for stacks allocation in automated container terminals. *Marit. Policy Manag.* **2023**, *50*, 1102–1117. [CrossRef]
2. Imai, A.; Nishimura, E.; Papadimitriou, S. Berth allocation with service priority. *Transp. Res. Part B Methodol.* **2003**, *37*, 437–457. [CrossRef]
3. Lin, X.; Pu, X.; Bai, X. On the efficiency impacts of berthing priority provision. *Transp. Sci.* **2024**, *58*, 578–596. [CrossRef]
4. Gao, Y.; Zhen, L.; Lu, H.; Xu, X. Ship Scheduling for Taicang Port. *Inf. J. Appl. Anal.* **2025**, *55*, 484–505. [CrossRef]
5. Ganji, F.; Gholami, S. Minimizing fuel emission by optimizing ship scheduling considering priorities and release times. *Int. J. Environ. Sci. Technol.* **2024**, *21*, 135–152. [CrossRef]
6. Yıldırım, M.S.; Aydın, M.M.; Gökkuş, Ü. Simulation optimization of the berth allocation in a container terminal with flexible vessel priority management. *Marit. Policy Manag.* **2020**, *47*, 833–848. [CrossRef]
7. Chen, X.; Yan, R.; Wu, S.; Liu, Z.; Mo, H.; Wang, S. A fleet deployment model to minimise the covering time of maritime rescue missions. *Marit. Policy Manag.* **2023**, *50*, 724–749. [CrossRef]
8. Lu, H.; Lu, X. Joint optimization of berths and quay cranes considering carbon emissions: A case study of a container terminal in China. *J. Mar. Sci. Eng.* **2025**, *13*, 148. [CrossRef]
9. Ursavas, E. Priority control of berth allocation problem in container terminals. *Ann. Oper. Res.* **2022**, *317*, 805–824. [CrossRef]
10. Jiang, S.; Liu, L.; Peng, P.; Xu, M.; Yan, R. Prediction of vessel arrival time to port: A review of current studies. *Marit. Policy Manag.* **2025**, *53*, 301–326. [CrossRef]
11. Wang, Z.; Cheng, J.; Hu, H. A proactive-reactive-based approach for continuous berth allocation and quay crane assignment problems with hybrid uncertainty. *J. Mar. Sci. Eng.* **2024**, *12*, 182. [CrossRef]
12. Zhen, L.; Wang, W.; Lin, S. Analytical comparison on two incentive policies for shore power equipped ships in berthing activities. *Transp. Res. Part E Logist. Transp. Rev.* **2022**, *161*, 102686. [CrossRef]
13. Song, Z.; Tang, W.; Zhao, R.; Zhang, G. Implications of government subsidies on ship companies' shore power usage strategies in port. *Transp. Res. Part E Logist. Transp. Rev.* **2022**, *165*, 102840. [CrossRef]
14. Peng, Y.; Li, X.; Wang, W.; Wei, Z.; Bing, X.; Song, X. A method for determining the allocation strategy of on-shore power supply from a green container terminal perspective. *Ocean Coast. Manag.* **2019**, *167*, 158–175. [CrossRef]
15. Zhang, Z.; Zhu, Y.; Zhu, J.; Huang, D.; Yin, C.; Li, J. Collaborative optimization of shore power and berth allocation based on economic, environmental, and operational efficiency. *J. Mar. Sci. Eng.* **2025**, *13*, 776. [CrossRef]
16. Wang, T.; Du, Y.; Fang, D.; Li, Z. Berth allocation and quay crane assignment for the trade-off between service efficiency and operating cost considering carbon emission taxation. *Transp. Sci.* **2020**, *54*, 1307–1331. [CrossRef]
17. Rodrigues, F.; Agra, A. Berth allocation and quay crane assignment/scheduling problem under uncertainty: A survey. *Eur. J. Oper. Res.* **2022**, *303*, 501–524. [CrossRef]
18. Zhen, L.; Zhuge, D.; Wang, S.; Wang, K. Integrated berth and yard space allocation under uncertainty. *Transp. Res. Part B Methodol.* **2022**, *162*, 1–27. [CrossRef]
19. Guo, L.; Zheng, J.; Du, J.; Du, J.; Gao, Z.; Fagerholt, K. Integrated planning of berth allocation, quay crane assignment and yard assignment in multiple cooperative terminals. *Transp. Res. Part E Logist. Transp. Rev.* **2024**, *183*, 103456. [CrossRef]
20. Zhang, Y.; Liang, C.; Shi, J.; Lim, G.; Wu, Y. Optimal port microgrid scheduling incorporating onshore power supply and berth allocation under uncertainty. *Appl. Energy* **2022**, *313*, 118856. [CrossRef]
21. Wang, Z.; Hu, H.; Zhen, L. Berth and quay cranes allocation problem with on-shore power supply assignment in container terminals. *Comput. Ind. Eng.* **2024**, *188*, 109910. [CrossRef]
22. Parise, G.; Parise, L.; Malerba, A.; Pepe, F.M.; Honorati, A.; Chavdarian, P.B. Comprehensive peak-shaving solutions for port cranes. *IEEE Trans. Ind. Appl.* **2016**, *53*, 1799–1806. [CrossRef]
23. van Duin, J.H.R.; Geerlings, H.; Verbraeck, A.; Nafde, T. Cooling down: A simulation approach to reduce energy peaks of reefers at terminals. *J. Clean. Prod.* **2018**, *193*, 72–86. [CrossRef]
24. Iris, Ç.; Lam, J.S.L. Optimal energy management and operations planning in seaports with smart grid while harnessing renewable energy under uncertainty. *Omega* **2021**, *103*, 102445. [CrossRef]
25. Yu, J.; Voß, S.; Song, X. Multi-objective optimization of daily use of shore side electricity integrated with quayside operation. *J. Clean. Prod.* **2022**, *351*, 131406. [CrossRef]
26. Dai, H.; Ma, J.; Yang, Y.; Sun, J.; Dai, Y. A bi-layer model for berth allocation problem based on proactive-reactive strategy. *Comput. Ind. Eng.* **2023**, *179*, 109200. [CrossRef]

Disclaimer/Publisher's Note: The statements, opinions and data contained in all publications are solely those of the individual author(s) and contributor(s) and not of MDPI and/or the editor(s). MDPI and/or the editor(s) disclaim responsibility for any injury to people or property resulting from any ideas, methods, instructions or products referred to in the content.